



GLOBAL JOURNAL OF SCIENCE FRONTIER RESEARCH: A
PHYSICS AND SPACE SCIENCE

Volume 20 Issue 13 Version 1.0 Year 2020

Type : Double Blind Peer Reviewed International Research Journal

Publisher: Global Journals

Online ISSN: 2249-4626 & Print ISSN: 0975-5896

Generation and Recombination Processes in Disordered Semiconductor Structures with Deep Centers

By Sergey V. Bulyarskiy

Institute of Nanotechnology of Microelectronics

Abstract- The article represents the physical processes and mechanisms that accompany the work of the real p-n-junction in disordered semiconductor structures with deep centers. A model for the transfer of electrons and holes in disordered semiconductors has been developed and expressions for the recombination rate have been obtained, which take into account the exchange of charge carriers between neighboring localized regions. The probability of electronic transitions is calculated. It takes into account the electron-phonon interaction and explains the rapid build-up of reverse currents as the applied voltage increases. The new model of recombination in space charge region of p-n-junction has been developed. This model made it possible to develop a new method for processing current-voltage characteristics and determining the parameters of recombination centers in semiconductor devices including electron-phonon interaction parameters.

Keywords: *p-n-junction; current-voltage characteristic; generation; recombination; electron transition probability; electron-phonon interaction.*

GJSFR-A Classification: FOR Code: 091306



Strictly as per the compliance and regulations of:



Generation and Recombination Processes in Disordered Semiconductor Structures with Deep Centers

Sergey V. Bulyarskiy

Abstract- The article represents the physical processes and mechanisms that accompany the work of the real p-n-junction in disordered semiconductor structures with deep centers. A model for the transfer of electrons and holes in disordered semiconductors has been developed and expressions for the recombination rate have been obtained, which take into account the exchange of charge carriers between neighboring localized regions. The probability of electronic transitions is calculated. It takes into account the electron-phonon interaction and explains the rapid build-up of reverse currents as the applied voltage increases. The new model of recombination in space charge region of p-n-junction has been developed. This model made it possible to develop a new method for processing current-voltage characteristics and determining the parameters of recombination centers in semiconductor devices including electron-phonon interaction parameters. The nature of the reverse and forward currents of p-n-junctions is studied as the basis for the operation of these devices. The mechanisms of formation of the reverse current of the p-n-junction were discussed and it was concluded that the current is determined by the generation with the participation of deep centers and electron-phonon interaction.

Keywords: *p-n-junction; current-voltage characteristic; generation; recombination; electron transition probability; electron-phonon interaction.*

1. INTRODUCTION

Models of generation and recombination in homogeneous semiconductor structures were created in fundamental works for microelectronics [1, 2]. The results of these works perfectly describe the current-voltage characteristics (CVC) of ideal structures with a depletion region and defects in this region, photoelectric processes involving defects, and other important phenomena in semiconductors. These works have numerous applications and an extensive bibliography of citations, for example [3]. Nevertheless, these works require refinement and development when disordering, strong electric fields, and electron-phonon interaction take place. Nanoscale disorder in diamond-like semiconductors can be caused by different factors. Artificial nanoscale disorder is obtained by forming an array of quantum wells, for example, in crystals based

on III-V solid solutions and other complex semiconductors, including those based on oxides. This process can be initiated, for example, by irradiation or ion implantation of a semiconductor and silicon too. Natural nanoscale disorder can also be due to different factors: compensation, structural damage, glass formation, high defect concentration[4]. Silicon contains a wide variety of defects, including vacancy-impurity complexes. Oxygen is an important impurity located at interstitial sites in the silicon lattice. Vacancies are easily trapped by oxygen atoms, leading to a formation of vacancy-oxygen (VO) complexes. Upon annealing, VO complex can combine with vacancy or interstitial oxygen to form more complicated complexes, such as V₂O, VO₂, VO₃, and so on [4]. Defects in semiconductor devices are studied by various methods, most of which use capacitance measurement. Current-voltage characteristics of p-n junctions with defects contain all information about defects and deep centers that they create. However, the analysis of these characteristics is poorly developed. This article partially fills this research gap.

Disorders in semiconductors accompanied by spatial localization of electronic states. As a result, to recombine, charge carriers must overcome a potential barrier; barriers overcome through tunnelling is referred to as the tunneling recombination. Transport models with allowance for disordering were proposed in [5, 6]. Generation and recombination are accompanied by electronic transitions between localized states. A good description of the experimental results cannot be made without taking into account the electron-phonon interaction, which increases the probability of the mentioned transitions. The probabilities of such transitions have been investigated by many authors [7-12], however, results that are easy to compare with experiment were obtained in [13] and they successfully explained various experimental results [13 - 17].

This work is a review in which the author strives to show what fundamental processes underlie the transport phenomena in disordered semiconductor nano- and microelectronics structures with structural defects that create deep centers. Much attention is paid to the current-voltage characteristics of p-n-junctions based on such semiconductors and practical methods for determining the parameters of defects in them.

Author: Institute of Nanotechnology of Microelectronics of the Russian Academy of Sciences (INME RAS), Leninskiy prospect, 32A, Moscow, 119991, Russia. e-mail: bulyar2954@mail.ru

II. GENERALIZED RECOMBINATION THEORY

A schematic diagram of recombination processes in nanoscale-disordered materials is shown in Fig. 1.

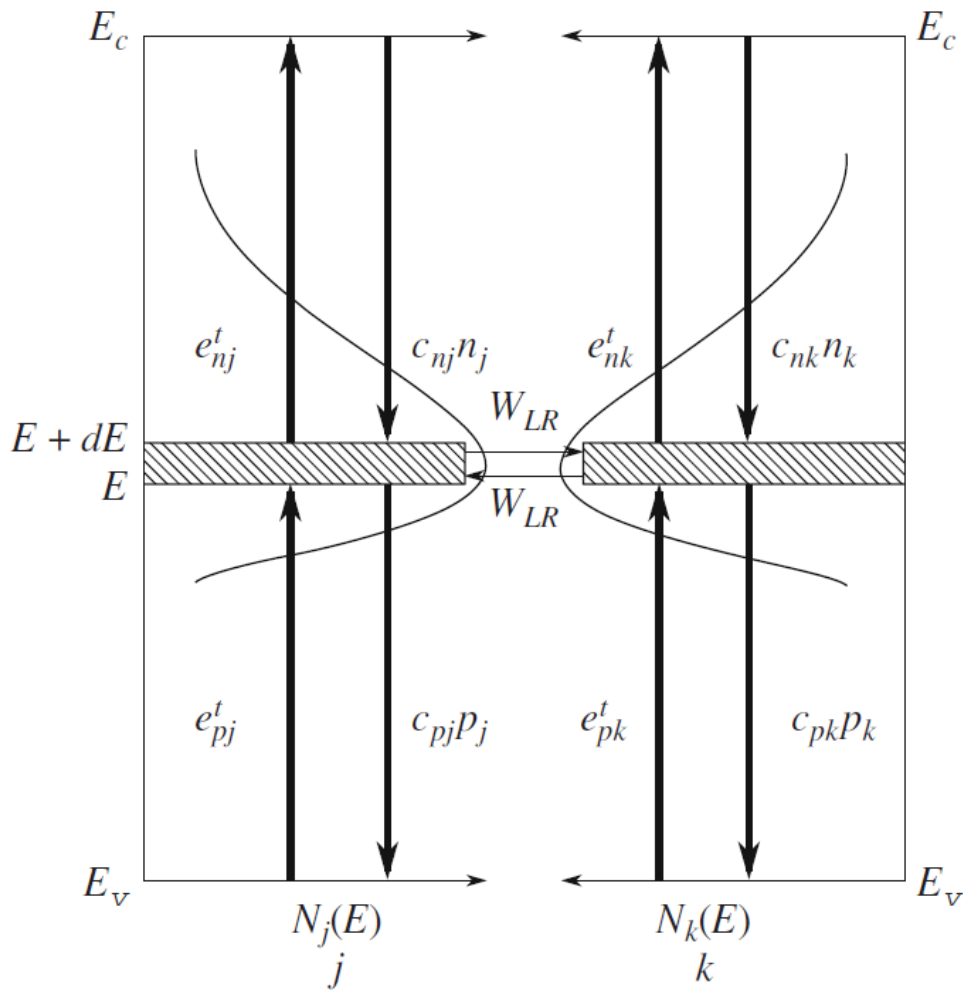


Fig. 1: Diagram of the recombination processes and electron transitions in our model

In accordance with this diagram, there are two regions in a semiconductor, separated by a potential barrier. Due to the nano scale disorder, localized states with different concentrations are formed in them, which can play the role of recombination centers. The barrier is tunnel-transparent between this regions. Recombination centers are present in each region, which are energy-distributed according to some (generally unknown) law. Recombination of charge carriers in each region may occur independently. There is also an additional mechanism of generation of non-equilibrium charge carriers, for example, injection.

Let us consider in more detail the model properties. We analyze a quasi-equilibrium stationary problem. Accordingly, both free and bound charge carriers have steady concentrations at each point of space. For various reasons (primarily, due to the spatially no uniform distribution of electric potential), these concentrations are different in each bound region. However, since quasi-equilibrium is established in the

system (tunneling, injection, and generation occur simultaneously), free charge carriers of each type are formed a unified subsystem. The electron and hole concentrations are generally different. A change in these concentrations is the sum of changes in the concentrations in all regions. Energy distribution of traps is determined by the physical features of nano scale disorder. They can be different in neighboring bound regions.

To calculate the total recombination rate, we will write the electron and hole recombination rates taking in to account the following:

1. The total recombination rate is determined by the recombination rates in all bound regions;
2. Localized states in each region are distributed over energies and characterized by both density and kinetic coefficients, which also have some energy distribution;

3. The occupation of localized states by charge carriers is generally described by not the Fermi-Dirac function, because the system is not in complete equilibrium but in a steady state;

therefore, this occupation function must be sought during the solution of the problem. The change in electron (n) and hole (p) concentrations in time t can be written as:

$$\frac{\partial n}{\partial t} = \int_E \left\{ -c_{nj}(E)n_j N_j(E)[1 - f_j(E)] - c_{nk}(E)n_k N_k(E)[1 - f_k(E)] + c_{nj}(E)n_{1j}(E)N_j(E)f_j(E) + c_{nk}(E)n_{1k}(E)N_k(E)f_k(E) \right\} dE, \tag{2.1}$$

$$\frac{\partial p}{\partial t} = \int_E \left\{ -c_{pj}(E)p_j N_j(E)f_j(E) - c_{pk}(E)p_k N_k(E)f_k(E) + c_{pj}(E)p_{1j}(E)N_j(E)[1 - f_j(E)] + c_{pk}(E)p_{1k}(E)N_k(E)[1 - f_k(E)] \right\} dE, \tag{2.2}$$

Where: $c_{nj,k}(E)$ & $c_{pj,k}(E)$ is the coefficient of electron & hole capture by localized states in the range between E and $E + dE$ in regions j and k : $n_{j,k}(p_{j,k})$ is the density of the electron concentration at the bottom of the conduction band (at the corresponding percolation level) or the hole concentration (at the top of the valence band or at the corresponding percolation level); $n_{1i,1k}(E) = N_c \exp[-(E_c - E)/kT]$ is a parameter characterizing the rate of electron emission; $p_{1j,1k}(E) = N_v \exp[-(E - E_v)/kT]$ is a parameter characterizing the rate of hole emission; E_c is the energy of the bottom of the conduction band (the corresponding percolation level); E_v is the energy of the

top of the valence band (the corresponding percolation level); $N_{j,k}(E)$ are the energy density distributions of the localized states in the j th and k th regions; $f_{j,k}(E)$ is the probability of electron occupancy of the localized states.

Eq. (2.1) and (2.2) include only thermal processes; however, it is not difficult to take into account optical processes, both between states inside the mobility gap and outside it.

1) The filling functions of the electronic states of defects differ from the Fermi-Dirac function and include the injection processes. We can show this if we equate Eq. (2.1) and Eq.(2.2), how it should be done in equilibrium. For the region J we have for example:

$$f_j(E) = \frac{\left\{ [c_{pj}(E)p_{1j}(E) + c_{nj}(E)n_j]N_j(E) + [c_{pk}(E)p_{1k}(E)]N_k(E) - [t_{nk}(E) + t_{pk}(E)]N_k(E)f_k(E) \right\}}{[t_{nj}(E) + t_{pj}(E)]N_j(E)}, \tag{2.3}$$

Where: $t_{nj,k}(E) = c_{nj,k}(E)[n_{j,k} + n_{1j,1k}(E)]$; $t_{pj,k}(E) = c_{pj,k}(E)[p_{j,k} + p_{1j,1k}(E)]$.

2) The probability of filling the traps is determined not only by vertical thermal and optical transitions, but also by horizontal ones between neighboring localized states. It is this fact that leads to a generalization of the theory of generation and recombination processes. We take into account the probability of transitions between localized states and thus include ballistic transfer, hopping conduction, and tunneling in the theory. This is

important for disordered semiconductors, when charge carriers are localized in a certain region, they cannot move freely along the semiconductor, the transition to an adjacent state occurs with a certain probability, which must be calculated separately. The conclusion of this statement was made in [5,6]. Here we give the result for the rate of change in the filling of localized states:

$$\begin{aligned} \frac{\partial n_{ij}}{\partial t} = & \int_E c_{nj}(E)n_j N_j(E) + c_{pj}(E)p_{1j}(E)N_j(E) - [t_{nj}(E) + t_{pj}(E)]N_j(E)f_j(E)dE - \\ & - \int_E \int_{E'} w_{LR}(E,E')N_j(E)f_j(E)N_k(E')[1 - f_k(E')]dEdE' + \\ & + \int_E \int_{E'} w_{RL}(E,E')N_j(E)[1 - f_j(E)]N_k(E')f_k(E')dEdE' \end{aligned} \tag{2.4}$$

Where: $w_{LR}(E)$ and $w_{RL}(E)$ are the probabilities of transition between neighboring regions. These probabilities include not only purely electronic transitions, but can take into account the interaction of charge carriers with the crystal lattice, which is expressed in the formation of polarons and is called the electron-phonon interaction. These expressions will be given below in the text.

The final expression for the recombination rate taking into account the transition between localized states [5,6] is:

$$R = R_j + R_k + R_{jk}, \tag{2.5}$$

Where: The rate of recombination in the region J:

$$R_j = \int_E \frac{c_{nj}(E)c_{pj}(E)(n_i^2 - p_j n_j)(T_{pnk} + w(E)N_j + AUN_j)N_j(E)}{T_{pnk}T_{pnj} + w(E)N_k T_{pnk} + w(E)N_j T_{pnj} + AUN_j T_{pnj}} dE,$$

The rate of recombination in the region K:

$$R_k = \int_E \frac{c_{nk}(E)c_{pk}(E)(n_i^2 - p_k n_k)(T_{pnj} + w(E)N_k)N_k(E)}{T_{pnk}T_{pnj} + w(E)N_k T_{pnk} + w(E)N_j T_{pnj} + AUN_k T_{pnk}} dE,$$

The rate of transition from the localized state of the region J to the region K and back:

$$R_{jk} = \int_E \frac{w(E)\{N_j N_k(E)D_{jk} + N_k N_j(E)D_{kj}\} + AU\{N_j N_k D_{jk}\}}{T_{pnk}T_{pnj} + w(E)N_k T_{pnk} + w(E)N_j T_{pnj} + AUN_j T_{pnj}} dE,$$

The designations used are:

$$D_{jk} = t_{nj}(E)c_{pk}(E)p_{1k}(E) - t_{pj}(E)c_{nk}(E)n_k,$$

$$D_{kj} = t_{nk}(E)c_{pj}(E)p_{1j}(E) - t_{pk}(E)c_{nj}(E)n_j.$$

This expression seems cumbersome and incomprehensible, but it can be easily converted into simple and understandable formulas:

a) Shockley recombination rate through deep traps

We assume that the recombination occurs in one region J, the transition probabilities $w_{LR}(E)$ and $w_{RL}(E)$ are equal to zero. Recombination is done through discrete levels ($N_{ij} = N_{ij}(E)\delta(E - E_{ij,k})$). We will take these remarks into account and obtain from Eq.(2.5) the well-known formula:

$$R = \frac{c_{nj}c_{pj}(p_j n_j - n_i^2)N_{ij}}{c_{nj}(n_{1j} + n_j) + c_{pj}(p_{1j} + p_j)} \tag{2.6}$$

b) Tunneling and tunneling recombination transport of charge carriers [5,6].

In most disordered semiconductors, electrons and holes are localized and spatially separated. Recombination can take place only if one of the stages of the process is tunneling and one of the charge carriers makes a jump into a new localized state. The charge carriers come to quasi-equilibrium after that. Hence the name of the model - tunneling recombination.

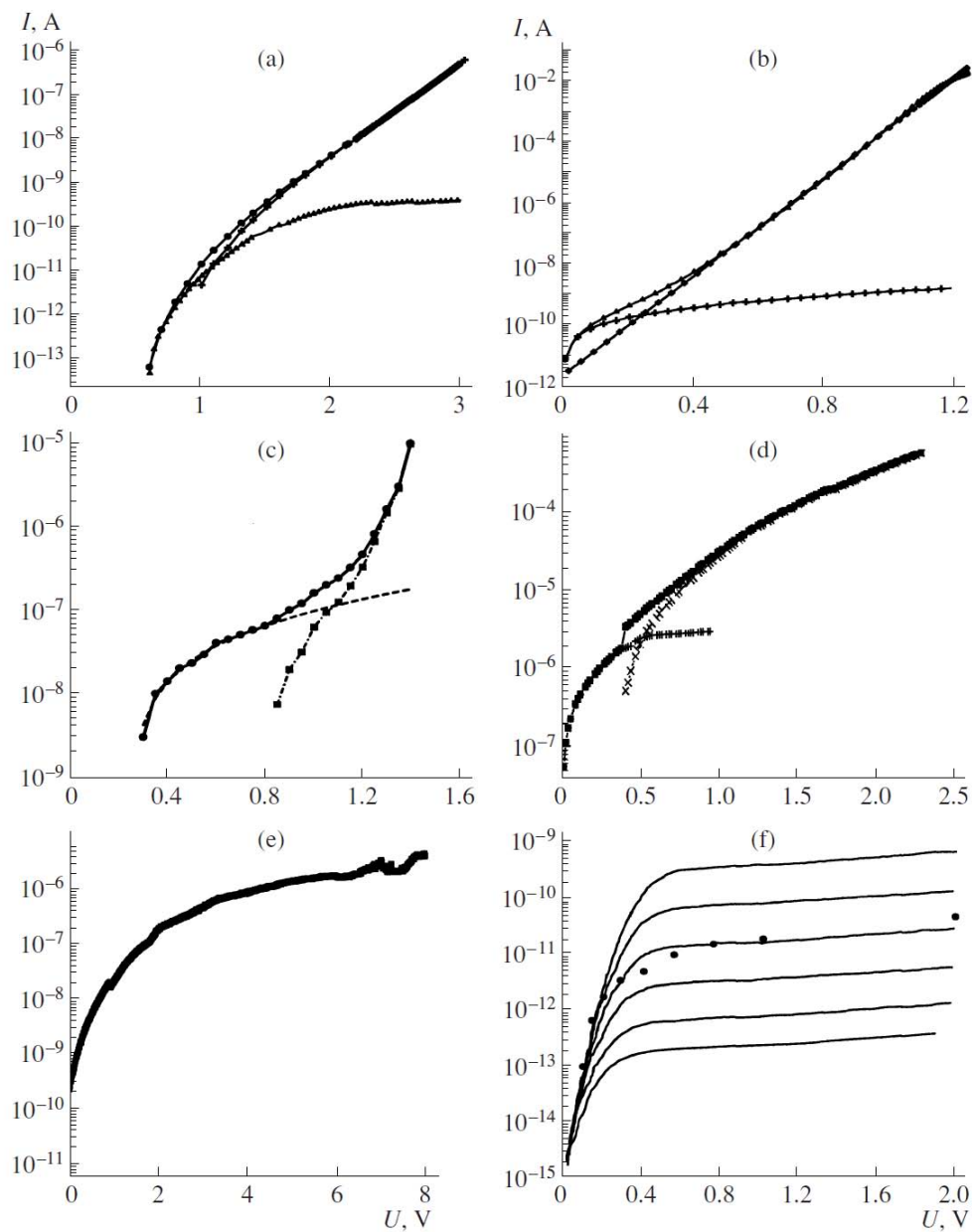


Fig. 2: Current-voltage characteristics of nanoscale disordered structures: (symbols) experiment and (lines) calculation from formula (2.7). (a) LEDs with a set of In GaN quantum wells, (b) GaAs LEDs with a high concentration of EL2 traps, (c) p-n junctions in Be-implanted GaP, (d) In/CdMnTe Schottky barriers, (e) Cu/TiGaSe₂ Schottky barriers, and (f) In/glassy As₂S₃ contacts.

The above-described exchange model also follows from formula (2.5). We will assume that in one region the traps exchange only with the electronic percolation level, and in the other, with the hole

percolation level. Assuming that $c_{pj} = 0$ and $c_{nk} = 0$, from Eq. (2.5) we obtain:

$$R = \int_E \frac{w(E)N_jN_k(E)c_{nj}(E)n_{1j}(E)c_{pk}(E)p_{1k}(E) - w(E)N_kN_j(E)c_{nj}(E)n_jc_{pk}(E)p_k + AUN_kN_j(E)t_n c_{pk} p_{1k}}{t_{pk}(E)t_{nj}(E) + w(E)N_k(E)t_{pk}(E) + w(E)N_jt_{nj}(E) + AUN_jt_{nj}} dE \quad (2.7)$$

Formula (2.7) can be used to describe various disordered semiconductors, as well as for ballistic transfer of charge carriers in carbon nano tubes.

Examples of application of Eq. (2.7) are in work [5], the results of which are shown in Fig. 2.

Formula (2.5) is general and can be used for almost all cases of carrier transfer between localized electronic states. This article is discussing the use of formula (2.5) for the analysis of generation and recombination processes in p-n-junctions with deep centers.

III. THE PROBABILITY OF ELECTRONIC TRANSITIONS BETWEEN LOCALIZED STATES TAKING INTO ACCOUNT THE ELECTRON-PHONON INTERACTION

The transition of a charged particle (electron or hole) between localized states causes a change in the electric field, which leads to the appearance of a polaron state and a change in lattice vibrations. This is the essence of the electron-phonon interaction, which

changes the probability of an electronic transition. Accurate calculations should take into account changes in the potential energy of the electron-crystal lattice system, the displacement of the atoms of the crystal lattice, which in turn leads to a change in the density of phonon states, etc. They are complex and cannot be used in practice. There is a simple one-coordinate model, which is similar to Einstein's model for thermal conductivity, it can be accurately calculated and fairly accurately describes the result of electron-phonon interaction. Ridley's book allows you to get acquainted with it in detail and understand the basic principles of the one-coordinate model [11]. This model is well represented by the configuration-coordinate diagram, which reveals the features of the electronic transition with electron-phonon interaction (Fig.3).

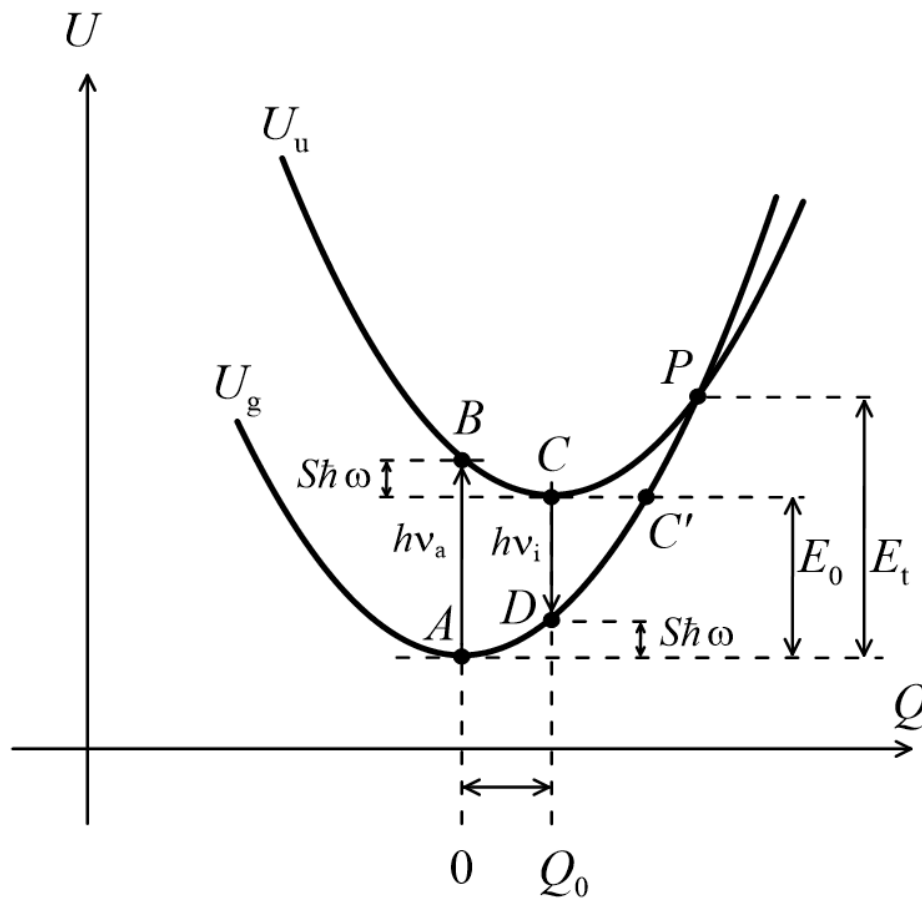


Fig. 3: Configuration-coordinate diagram

We will talk about an electron that passes between localized states, but all our reasoning is valid for a hole. The construction of such a diagram is based on a simplified approximation of the one-coordinate model, according to which the ground and excited states of the centers are described by adiabatic potentials, the energy of which is proportional to the square of a certain generalized coordinate \$Q\$. When the system passes from the ground state to the excited one,

the polaron effect takes place, as a result of which the adiabatic potential of the excited state is shifted relative to the main potential by the amount \$Q_0\$ (polaron shift) and they intersect at point P (Fig 3.)

$$U_g = \frac{\hbar\omega Q^2}{2}; \quad U_u = \frac{\hbar\omega(Q-Q_0)^2}{2} + E_0 \quad (3.1)$$

Where: Q is generalized coordinate; $Q_0 = \sqrt{2S}$, $S\hbar\omega$ is a value equal to half of the heat release that accompanies the electron-phonon interaction; E_0 is the energy of a purely electronic transition, S is the Huang and Rees factor, $\hbar\omega$ is the energy of the characteristic phonon in the one-coordinate model; U_g is the adiabatic potential of the ground state of a center, U_u is the adiabatic potential of the excited state of a center, $h\nu_a$ is the energy of the absorption maximum during the transition from the ground state to the excited state, $h\nu_i$ is the energy of the maximum radiation during the transition from the excited state to the ground state, E_t is the energy of thermal activation.

$$E_t = \frac{(E_0 + S\hbar\omega)^2}{4S\hbar\omega}; \quad h\nu^{abc} = E_0 + S\hbar\omega, \quad (3.2)$$

$$h\nu^{em} = E_0 - S\hbar\omega,$$

This model is used to describe the possibility of multi phonon non-radiative transitions of charge carriers and avoids the difficulties of explaining the simultaneous interaction of many particles. With a non-radiative transition from the ground state (point A in Fig. 3) to an excited one (point C, Fig. 3), the system absorbs one phonon after another, while increasing the amplitude of the generalized coordinate. The transition itself occurs at the saddle point (point P, Fig. 3), when the energy of the ground state takes on the value E_t , and then the system relaxes to point C, also emitting phonons one after another to reduce the energy.

The probability W of transition between unperturbed states 1 and 2 is determined by the square of the absolute value of the matrix element \hat{H}' of the perturbation operator causing the transition:

$$W = \frac{2\pi}{\hbar} \left| \langle 1 | \hat{H}' | 2 \rangle \right|^2 \quad (3.3)$$

The exact calculation of this probability was made in [12, 13], its result is that for the probability of a quantum-mechanical transition, taking into account the electron-phonon interaction, in general form, it can be written as:

$$W = \sum_{i,j} \int_{-\infty}^{\infty} W_{0i,j}(E_{ii,j} - \varepsilon) f_{i,j}(\varepsilon) d\varepsilon, \quad (3.4)$$

Where: $W_{0i,j}(E_{ii,j} - \varepsilon)$ is the probability of a purely electronic transition from i - the sublevel of the multiplet of the initial state of the center to j - the sublevel of the final state of the multiplet, $f_{i,j}(\varepsilon)$ is the expression for the shape function of the optical transition from - the sublevel of the multiplet of the initial state of the center

to i - the sublevel of the final state j of the multiplet, $\sum_{i,j}$ is summation over all sublevels of the multiplets 1 and 2.

Eq.(3.4) is common for transitions between different localized states. It can be used for multiphonon thermal, tunneling, and optical transitions. Probability of a purely electronic transition $W_{0i,j}(E_{ii,j} - \varepsilon)$ is presented in numerous monographs, including [11]. The shape function that reflects the electron-phonon interaction can be calculated from experiments on radiation or energy absorption during transitions with the participation of deep centers [12, 13]. This is often difficult. Therefore, this function can be approximated by the Gauss normal distribution:

$$f_{i,j}(\varepsilon) = \frac{1}{\sigma\sqrt{2\pi}} \exp\left[-\frac{(\varepsilon - E_0)^2}{2\sigma^2}\right]; \quad \sigma = \sqrt{2S\hbar\omega kT} \quad (3.5)$$

The parameters of the function forms can be found by analyzing the current-voltage characteristics. This important and interesting method will be discussed below.

IV. RECOMBINATION IN THE DEPLETION REGION OF THE P-N JUNCTION AT FORWARD BIAS VOLTAGE. RECOMBINATION SPECTROSCOPY

The recombination in the space charge region (SCR) determines the current-voltage characteristics (CVC) of almost all semiconductor devices with a low injection level, which occurs at low forward bias voltages at the p - n -junction. This section begins near zero voltage and lasts up to a voltage of the order of the diffusion potential, which, as is well known, characterizes a potential barrier in the contact area at zero displacement. The main results of this chapter were partially obtained earlier [18-22]. In an ideal diode, it is assumed that there are no generation-recombination processes in the space charge region (SCR) and the current through the p - n -junction is determined by carrier injection through the barrier. The equation of the Current-Voltage characteristic (CVC) has the form:

$$j = j_s \left[\exp\left(\frac{qU}{mkT}\right) - 1 \right] \quad (4.1)$$

Where: j_s is revers saturation current density; U is a voltage on the p - n -junction; k is the Boltzmann constant; q is electron charge; m is the ideality factor.

Ideality factor (m) has the meaning 1 in the Shockley's diffusion theory [1] and 2 in the model generation and recombination in p - n -junctions [2]. The revers saturation current density is associated with the parameter lifetime (τ) in last model and it is a display in

the form: $j_s = j_{s0} / \tau$. Classical reverse current does not depend on voltage. The dependence of the current on the voltage takes place in the so-called short-base diodes, when the base thickness is of the order of the diffusion length.

Scientific articles do not consider the problem that the ideality factor and the lifetime can depend on the voltage applied to the p-n-junction. Such an understanding of these values is not true, since the voltage value changes the flow of injected charge carriers. Ideality factor and the lifetime should change with a change in bias voltage too, because they depend on the injection. Numerous training courses and lectures do not pay enough attention to this problem.

The CVC during recombination in the SCR was obtained in [25] and can be represented as:

$$I = \frac{qAw(U)n_i}{2\tau} \left(\exp\left(\frac{qU}{2kT}\right) - 1 \right) \quad (4.2)$$

$$n(x) = n_n \exp\left(-\frac{\phi(x)}{kT}\right), \quad p(x) = p_p \exp\left(-\frac{q(V_d - U) - \phi(x)}{kT}\right). \quad (4.3)$$

Where: $\phi(x)$ is potential of semiconductor structure at point x. Eq.(4.3) must be substituted into Eq. (2.6), then we obtain an important formula for CVC, the derivation and application of which is described in detail in [18 - 22]:

$$I_r = qA \int_{-x_p}^{x_n} R(x) dx \approx \frac{qAR_{\max}w}{2}, \quad (4.4)$$

$$R_{\max} = \frac{c_n c_p n_i^2 N_t \left[\exp\left(\frac{eU}{kT}\right) - 1 \right]}{2n_i \sqrt{c_n c_p} \exp\left(\frac{eU}{2kT}\right) + c_n n_1 + c_p p_1} \quad (4.5)$$

$$I_r(U) = qAw(U) \cdot \frac{c_n c_p n_i^2 N_t (e^{qU/kT} - 1)}{2n_i \sqrt{c_n c_p} e^{qU/2kT} + c_n n_1 + c_p p_1} \cdot \frac{2kT}{e(V_d - U)} \quad (4.6)$$

Where: V_d is the diffusion potential of the p-n junction.

$$m = \frac{e}{kT} \left(\frac{d \ln I_r}{dU} \right)^{-1} = \frac{eI_r}{kT} \left(\frac{dI_r}{dU} \right)^{-1} \quad (4.7)$$

The current-voltage characteristic, the rate of recombination in the space-charge region, and the differential slope depend on the parameters of the recombination centers with deep levels in the band gap of the semiconductor and the voltage at the p-n-junction

where $w(U)$ is the width of the SCR of the p-n junction; n is a concentration of intrinsic charge carriers; A is the area of the p-n junction, τ is the lifetime of non-equilibrium charge carriers. The differential slope in this case is 2. Such an expression for recombination in the SCR was obtained under the simplifying assumption that the capture coefficients at the recombination center are equal for electrons and holes.

The recombination rate from Shockley's theory Eq.(2.6) allows one to obtain a more accurate expression for the current-voltage characteristic, from which it follows that the differential slope and the lifetime depend on the number of charge carriers injected into the SCR, and, consequently, on the forward bias voltage. The concentration of free carriers in the SCR can be obtained by multiplying the concentration of free carriers in the corresponding region by the Boltzmann factor, taking into account the influence of the electric field of the p-n-junction. These concentrations are calculated by the formulas in a one-dimensional model:

[15]. Therefore, the parameters of deep levels can be calculated from the CVC. We will do this using the example of deep centers in silicon p-i-n structures [16]. The calculation results of β for the diodes that were studied are shown in Fig. 6.

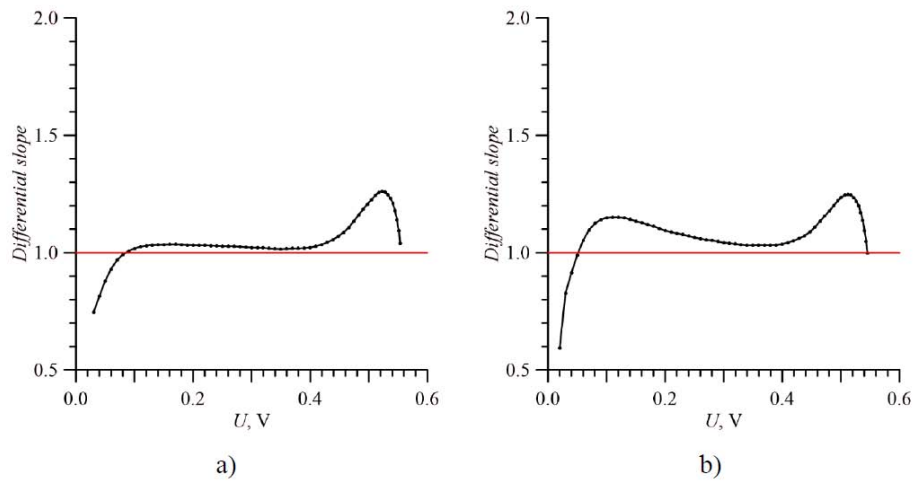


Fig. 4: Differential slope of the forward CVC of the diodes at room temperature

a) before irradiation; b) after irradiation [16].

The experimental results of Fig. 4 show that the values of the differential slope are in the range $1 < \beta < 2$. The value of β exceeds 1 after irradiation more significantly. According to the results of [20, 21], the presence of maxima in the dependence of the differential slope on the forward bias voltage indicates the existence of recombination centers. The differential slope shows two maximum (see Fig. 4), the first of which is blurred, which may be due to the influence of several recombination centers. These facts indicate that the direct CVC is determined by recombination in the SCR.

The experimental CVC underwent a transformation, which made it possible to better reveal their features. The dependence of a certain quantity on the forward bias voltage was calculated, which was called the reduced recombination rate ($R(U) \eta p$). This value is the inverse of the lifetime and has features that are associated with the parameters of recombination centers. The reduced recombination rate is defined as [22]:

$$R_{pr} = \frac{I_r(U)}{eSw(U)n_i \left[\exp\left(\frac{eU}{2kT}\right) - 1 \right]} \frac{e(V_d - U)}{2kT} = \frac{c_n c_p n_i N_t \left[\exp\left(\frac{eU}{2kT}\right) + 1 \right]}{2n_i \sqrt{c_n c_p} \exp\left(\frac{eU}{2kT}\right) + n_1 c_n + p_1 c_p} \quad (4.8)$$

The dependence of the reduced recombination rate on the bias voltage is shown in Fig. 5. This curve consists of two sections. Eq. (4.8) is described by the following dependency, then

$$2n_i \sqrt{c_n c_p} \exp\left(\frac{eU}{2kT}\right) < n_1 c_n + p_1 c_p :$$

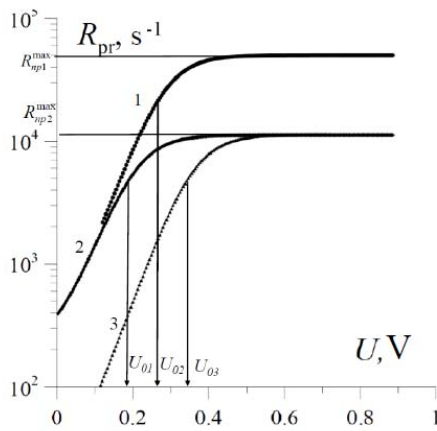
$$R_{pr} = c_p \left(\frac{m_p^*}{m_n^*}\right)^{3/4} N_t \exp\left(-\frac{E_g - E_m}{kT}\right) \exp(eU/2kT). \quad (4.9)$$

Eq. (4.8) is described by the following dependency, then: $2n_i \sqrt{c_n c_p} \exp\left(\frac{eU}{2kT}\right) > n_1 c_n + p_1 c_p :$

$$R_{pr} = R_{pr}^{\max} = \sqrt{c_n c_p} N_t / 2. \quad (4.10)$$

We will define the value of U_0 as the voltage at which the condition ($R_{pr} = R_{pr}^{\max} / 2$) is satisfied, then $c_n n_1 + c_p p_1 = 2n_i \sqrt{c_n c_p} \exp\left(\frac{eU_0}{2kT}\right)$. We will assume that the energy of the recombination center lies above the middle of the forbidden band, i.e., $c_p p_1 \ll c_n n_1$ and we find:

$$E_m = \frac{E_g - eU_0}{2} + \delta, \text{ where: } \delta = \frac{kT}{2} \ln\left(\frac{1}{4} \frac{c_n N_c}{c_p N_v}\right). \quad (4.11)$$



$$c_n / c_p : 1 - 1; 2 - 10; 3 - 0.1.$$

Fig. 5 is showing the results of the simulation of the reduced recombination rate for various ratios of the values of the capture coefficients. We took into account that the correction is equal to 0.01 eV for the ratio of the ratio of the effective masses of silicon and can be neglected. The ratio of the capture rate constant coefficients can introduce a certain systematic error. For calculations Fig. 6 this value is 0.06 eV. The reduced recombination rate must be measured at several temperatures to avoid this error. The results are shown in Fig. 6. to simulate the reduced recombination rate at different temperatures. The temperature dependence ($R_{np} = f(1/T)$) at a fixed bias voltage (U_t) is shown in Fig. 7 [15].

Fig. 5: Modeling the reduced recombination rate for a recombination center with an activation energy of 0.4 eV and three ratios of capture coefficients

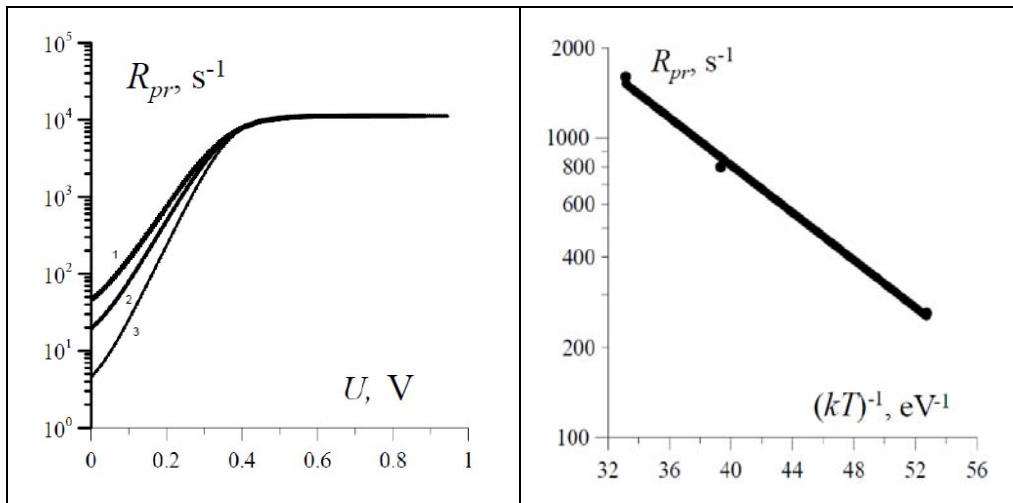


Fig. 6: Modeling the reduced recombination rate of a deep center with activation energy of 0.4 eV at different temperatures [15] T , K: 1 - 350; 2- 295; 3 - 220.

Fig. 7: Temperature dependence of the of reduced recombination rate at $U = 0.1 V$ [15].

The activation energy of this straight line is equal to ($E_A = 0.5E_g - E_m - eU_1$) and allows you to calculate the activation energy of the recombination center.

$$E_m = 0.5E_g - E_A - eU_1 \quad (4.12)$$

The activation energy, which was obtained as a result of the calculation, is equal to the energy of 0.4 eV, at which the simulation was performed.

Thus, the study of temperature dependences allows us to accurately estimate the activation energy, and then the ratio of the capture rate constants using Eq. (4.12). Calculate the ratio of the capture rate constant coefficients by the formula, if you know the voltage at which the reduced recombination rate is halved (U_0), and the level of thermal activation energy:

$$\frac{c_n}{c_p} = 4 \left(\frac{m_p^*}{m_n^*} \right)^{3/2} \exp \left[\frac{(eU_0 + 2E_m - E_g)}{kT} \right]. \quad (4.13)$$

If the ratio of the capture rate constant coefficients (c_n/c_p) is known (from other experiments or calculations), then it is possible to calculate the lifetimes in the heavily doped n-type material for the p-type:

$$\tau_{po} = (c_p N_t)^{-1} = \frac{1}{2} \sqrt{\frac{c_n}{c_p}} (R_{pr}^{max})^{-1},$$

$$\tau_{no} = (c_n N_t)^{-1} = \frac{1}{2} \sqrt{\frac{c_p}{c_n}} (R_{pr}^{max})^{-1}. \quad (4.14)$$

Eq. (4.14) allows us to conclude that the temperature dependences of the reduced

recombination rate are determined by the lifetime of charge carriers. We can construct a diagram that shows the relationship between the lifetime with the temperature of the experiment and the level of injection if we use Eq.(4.12) and Eq.(4.14) and the results of the experiment at different and sufficiently close to each other temperatures. This was done in article [23]. We can represent expressions Eq.(4.8) - (4.11) as a function of the lifetimes of electrons and holes when captured by the recombination center Ex.(4.14):

$$R_{pr} = \frac{\frac{\tau_{n0}^{-1}\tau_{p0}^{-1}}{N_t} n_i \left[\exp\left(\frac{qU}{2kT}\right) + 1 \right]}{\frac{2n_i \sqrt{\tau_{n0}^{-1}\tau_{p0}^{-1}}}{N_t} \exp\left(\frac{qU}{2kT}\right) + c_n n_1};$$

$$R_{prS} \approx \tau_{n0}^{-1}\tau_{p0}^{-1}/2; R_{pr} \approx \frac{1}{\tau_{p0}} \frac{n_i^2}{n_1} \left[\exp\left(\frac{qU}{2kT}\right) + 1 \right]. \quad (4.15)$$

Eq. (4.15) are the basis for calculating the parameters of the recombination center. The calculation algorithm is as follows: by Eq. (4.11) we determine the activation energy of the recombination center; we select a certain point with coordinates on the dependence of the reduced recombination rate, then solving the system of Eq. (4.15) together, we obtain the following relations for the characteristic lifetimes:

$$\tau_{n0}^{-1} = \frac{4R_{prS}^2 n_i}{n_1 R_1} \exp\left(\frac{U_1}{2kT}\right);$$

$$\tau_{p0}^{-1} = \frac{n_1 R_1}{n_i} \exp\left(-\frac{U_1}{2kT}\right); \frac{c_p}{c_n} = \frac{n_1^2 R_1^2}{4R_{prS}^2 n_i^2} \exp\left(\frac{eU_1}{kT}\right) \quad (4.16)$$

The calculation results are shown in Fig. 7 [23]

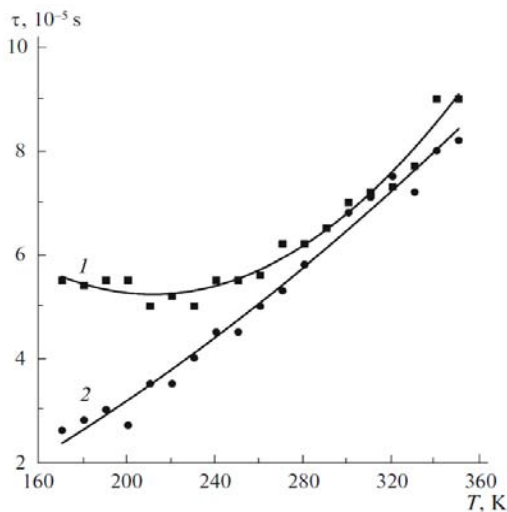


Fig. 8: Temperature dependence of the lifetime through levels with activation energy, eV: 0.45 (1); 0.39 (2).[23].

In order to select areas (in space of the forward bias voltage - the temperature) in which the recombination fluxes pass through these or those centers, we will proceed as follows:

- Plot the temperature dependences of the forward current at various forward bias voltages in the coordinates of Arenius;
- Select straight sections on them and calculate the activation energies;
- Calculate the activation energies of deep centers by Eq.(4.12).

Thus, by finding the activation energy at different bias voltages and temperatures, one can roughly single out the regions where recombination through one or another center predominates. Such a diagram is plotted in Fig. 9.[23].

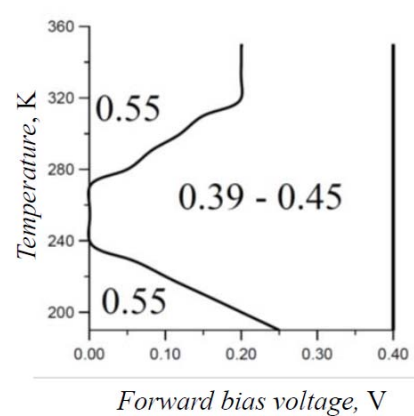


Figure 9: Regions in space of temperatures and forward bias voltages in which recombination through one center or another prevails. The energies of the recombination centers are shown in the figure in eV [23].

Recombination through levels with an activation energy of 0.55 eV prevails in two regions at low temperatures and low biases and at high temperatures and high biases. In the remaining region, recombination dominates through levels with activation energies of 0.39 and 0.45 eV. This behavior of recombination flows is not random. For the 0.55 eV level, in the indicated regions, the lifetime decreases rapidly and it intercepts recombination fluxes. According to Fig. 9. The lifetime for recombination through the levels of 0.39 and 0.45 eV in the region of small displacements increases rapidly. This is due to the fact that in this voltage region the injection level is still small, and the processes of emission from these centers prevail over the processes of capture.

Several recombination centers can exist simultaneously in a semiconductor and the recombination processes with their participation proceed in parallel and independently from each other [16-23]. Recombination currents are added to the total current additively. At the same time, the real dependence is the sum of these processes. The

recombination process proceeds with the participation of three recombination levels belonging to independent recombination centers. This dependence can be expressed by the formula:

$$R_{pr}(U) = \sum_k \frac{c_{nk}c_{pk}n_iN_{tk} \left[\exp\left(\frac{eU}{2kT}\right) + 1 \right]}{2n_i\sqrt{c_{nk}c_{pk}} \exp\left(\frac{eU}{2kT}\right) + c_{nk}n_{1k} + c_{pk}p_{1k}} \quad (4.17)$$

The algorithm for dividing an experimental curve into components is based on analytical approximations Eq. (4.15) as well as on the following provisions:

1. The Current-Voltage characteristic of a directly biased *p-n*-junction is measured at voltages less than the diffusion potential (V_d). Note that the measurement points should be quite a lot. The reduced recombination rate (R_{pr}) is calculated for each voltage using Eq. (4.8). The width of the space charge region ($w(U)$) and the diffusion potential (V_d) are calculated from capacitive measurements.
2. We build a dependency $\ln(R_{pr}(U))$ graph and graphically decompose this dependency into its components.. Each component of the reduced recombination rate has a saturation, the value of which is determined by Eq. (4.8). In the initial area $R_{pri}(U)$ there is a change according to the law $\exp(eU/2kT)$ Eq.(4.83).
3. We find U_{0i} for each curve that characterizes recombination through a single level. Then we estimate the activation energy of the corresponding

deep center by the Eq. (4.11), neglecting the value δ . The systematic error, which is associated with neglect δ , is determined by the ratio of the capture rate constant coefficients (c_n / c_p) and, as a rule, has amounts about 0.05 eV at $T = 300$ K.

Thus, the formulas and calculation algorithm for simple recombination processes can be applied after the separation of complex processes into components.

Thus, one can approximately find the parameters of deep centers from current-voltage and voltage-farad measurements at each fixed temperature. These measurements can be made even on a semiconductor wafer and carry out the screening of diodes on the basis of the presence of deep centers even before dividing the wafer into separate semiconductor devices.

V. DETERMINATION OF THE PARAMETERS OF THE ELECTRON-PHONON INTERACTION BY ANALYZING THE TEMPERATURE DEPENDENCES OF DIRECT CURRENTS.

The analysis of current-voltage characteristics does not allow calculating the concentration of recombination centers, but this can be done by the thermostimulated capacitance (TSC) or DLTS methods. The lifetime of electrons and holes during capture at the recombination center is related to the concentration of deep centers and the coefficients of capture of electrons and holes at the center using the relations:

$$\tau_{po} = (c_p N_t)^{-1} = \frac{1}{2} \sqrt{\frac{c_n}{c_p} (R_{np}^{\max})^{-1}}, \quad \tau_{n0} = (c_n N_t)^{-1} = \frac{1}{2} \sqrt{\frac{c_p}{c_n} (R_{np}^{\max})^{-1}} \quad (5.1)$$

The current-voltage characteristics were measured in the range of 290–343 K [15].

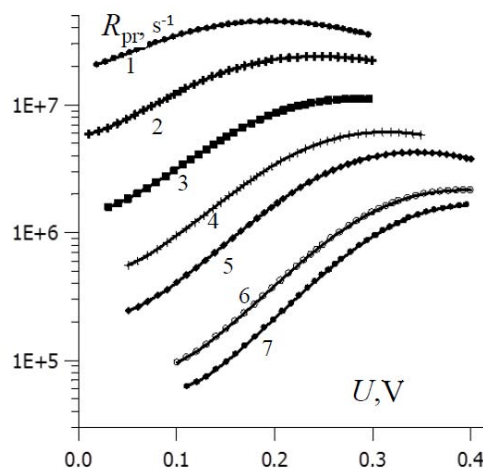


Fig. 10: Temperature dependence of the superficial recombination rate, T , K: 1 – 343; 2 – 333; 3 – 323; 4 – 313; 5 – 303; 6 – 294; 7 – 290 [15]

The temperature dependences of the reduced recombination rate are shown in Fig. 10. The strong temperature dependence of the saturation region of a given value takes place. The separation of the reduced recombination rate into components was done for each temperature independently and the capture rate

constant coefficients of holes and electrons for them were calculated. The results of the calculations are shown in Fig. 11 at the normal scale, and in fig. 12 - semi-logarithmic. In addition, analytical approximations are defined for all capture rate constant coefficients in the form:

$$c_i = c_{0i} \exp\left(-\frac{E_{bi}}{kT}\right)$$

$$E_t = 0.53\text{eV} \left\{ \begin{array}{l} c_n = 8.6 \exp\left(-\frac{0.30}{kT}\right) \\ c_p = 1.9 \cdot 10^8 \exp\left(-\frac{0.85}{kT}\right) \end{array} \right\} \quad E_t = 0.45\text{eV} \left\{ \begin{array}{l} c_n = 0.022 \exp\left(-\frac{0.16}{kT}\right) \\ c_p = 10^3 \exp\left(-\frac{0.57}{kT}\right) \end{array} \right\} \quad (6.1)$$

Where: E_{bi} is energy of nonradiative transition from excited to ground states.

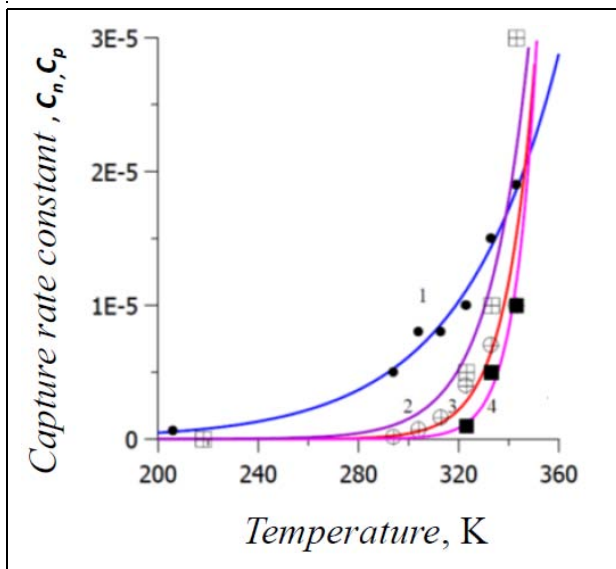


Fig. 11: Temperature dependences of the capture rate constant coefficients of deep centers with activation energies [15]:

2, 4 - 0.53eV; 1,3 - 0.45 eV.

1,2- C_n ; 3,4- C_p .

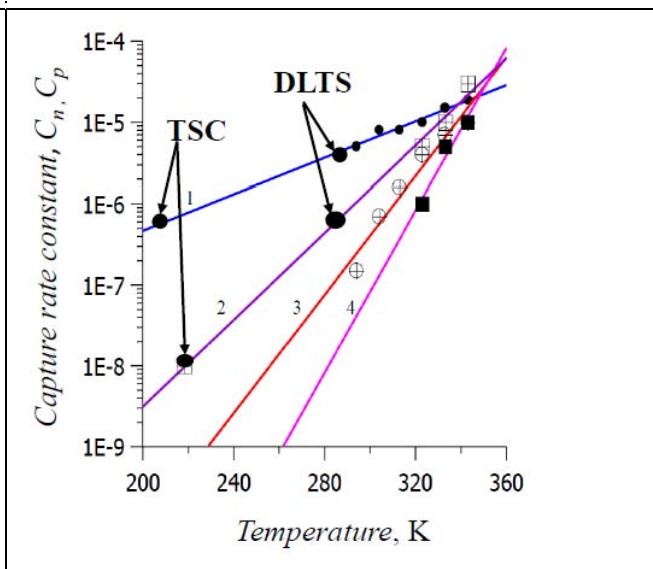


Fig. 12: Temperature dependences of the capture rate constant coefficients of deep centers with activation energies [15]:

2, 4 - 0.53eV; 1,3 - 0.45 eV.

1,2- C_n ; 3,4- C_p .

The results of measuring the capture rate constant coefficients by various methods are consistent with each other. The capture rate constant coefficients, which were calculated from the TSC and DLTS experiments, are less than the results of calculations from the current-voltage characteristics. This fact is due to the strong temperature dependence of these coefficients and the fact that they were measured at different temperatures. The temperature at which these coefficients were calculated from TSC experiments is the lowest, so their value is the smallest. The agreement of the results is there shows the correctness of the used models, experiments and calculations.

To determine the parameters of the electron-phonon interaction, we use the characteristic energies of non-radiative transitions[15]. This energy corresponds to the energy in the configuration diagram. It is associated with the parameters of the electron-phonon interaction as follows:

$$E_{Bi} = \frac{(E_0 - s\hbar\omega)^2}{4 s\hbar\omega} \quad (6.2)$$

Where: S is Huang and Rhys factor, which is equal to the number of phonons involved in the electron-vibrational transition; $s\hbar\omega$ is heat release in the theory

of electron-phonon interaction. This value is equal to the energy that is transmitted to the lattice during the non-radiative capture of an electron or hole to a deep center.

We will take the energy that must be expended for the non-radiative ejection of an electron from a deep center as the second quantity to be calculated. These energies were determined experimentally from current-voltage characteristics and are 0.45 and 0.55 eV. In the configuration diagram, they correspond to the energy E_{ij} . In our notation, this value, and it is associated with the parameters of the electron-phonon interaction as follows:

$$E_{ij} = E_0 + E_B = \frac{(E_0 + s\hbar\omega)^2}{4 s\hbar\omega}. \tag{6.3}$$

We get the desired parameters when we decide together Eq.(6.2) and Eq.(6.3):

Table 1: Parameters of deep centers taking into account the electron-phonon interaction

N _z	E_{np} , eV	E_{pb} , eV	E_{n0} , eV	E_{p0} , eV	E_{Bn} , eV	E_{Bp} , eV
1	0.45	2.8	0.29	0.83	0.16	0.57
2	0.53	6.2	0.23	0.89	0.30	0.85
	$s\hbar\omega$, eV		N_t , cm ⁻³	C_{n0} , cm ³ s ⁻¹	C_{p0} , cm ³ s ⁻¹	σ , eV
1	0.073		3*10 ¹¹	0.022	1000	0.061
2	0.082		4*10 ¹¹	8.6	1.9*10 ⁸	0.065

Table1 represents a complete set of parameters for two deep centers that allow one to calculate all the thermal, optical, and field dependences of deep centers.

VI. ANALYSIS OF CURRENT-VOLTAGE CHARACTERISTICS BY THE EXAMPLE OF THE SILICON PHOTODETECTORS BEFORE AND AFTER IRRADIATION

Forward and reverse CVC before and after irradiation of the silicon photo detectors are shown in Figure 13 [16]. In the initial section of the CVC with forward bias, an increase in current was observed after irradiation. Since the current in this region is due to recombination in the SCR, we can conclude that the concentration of recombination centers increases. Reverse current also increased. The current through the diode at the reverse bias is due to generation in the SCR and is proportional to the concentration of recombination centers. The generation current after irradiation increased 10 times. It can be assumed that the concentration of recombination centers increased 10 times after irradiation.

$$s\hbar\omega = \left(\sqrt{E_{ij}} - \sqrt{E_B} \right)^2$$

$$E_0 = \left(\sqrt{E_{ij}} - \sqrt{E_B} \right) \left(\sqrt{E_{ij}} + \sqrt{E_B} \right) \tag{6.4}$$

$$\sigma = \sqrt{2kT s\hbar\omega}. \tag{6.5}$$

Thus, the strength of the electron-phonon interaction is mainly determined by heat generation and leads to an increase in the emission rate in an electric field.

The results of calculations and experiments performed on two recombination centers are summarized in Table. 1

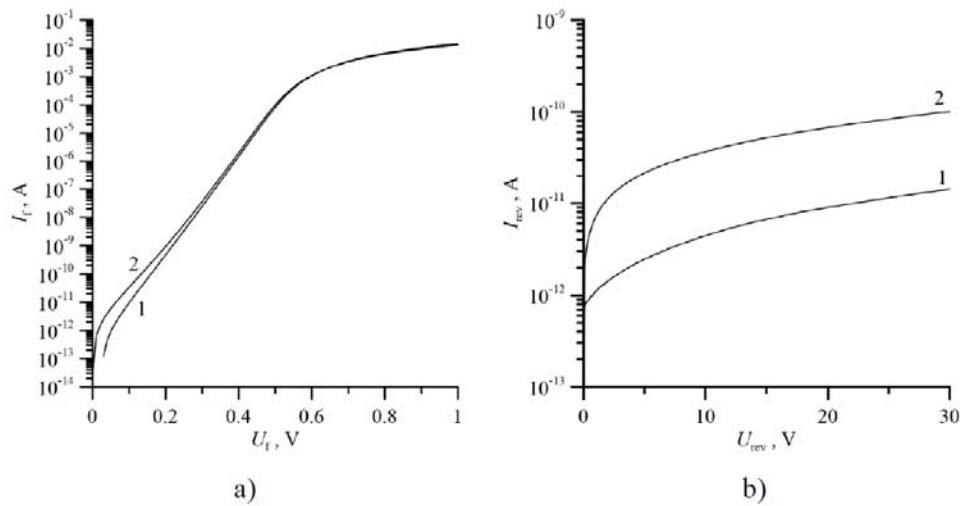


Figure 13: Forward (a) and reverse (b) current-voltage characteristics at room temperature before (1) and after (2) irradiation [16]

Reverse CVC plotted in coordinates $\ln(I) = f(F^{1/2})$ (where F is the electric field strength in the SCR of the diode) are linear (see Fig. 14). These facts indicate that the current through the diode at the

reverse bias is caused by generation and the Poole-Frenkel effect takes place, which lowers the height of the generation barrier in proportion to the root of the electric field strength [15].

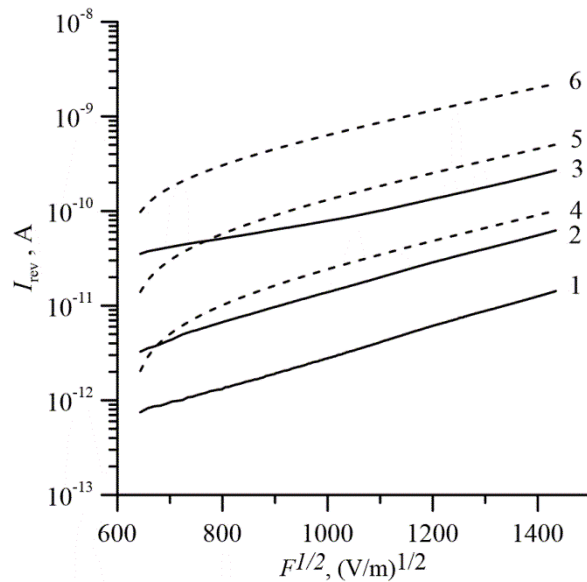


Figure 14: CVC plotted in Poole-Frenkel coordinates before irradiation (1,2,3) and after irradiation (4,5,6) measured at temperatures [16], °C: 1,4 - 0; 2,5 to 20; 3,6 -4.0

The temperature dependences of the reverse current plotted in the Arrhenius coordinates for various reverse bias voltages on the diode (see Fig. 15) allow us to determine the generation energies of charge carriers at various electric field strengths in the SCR of the p-n junction. We must pay attention to the fact that the energies that are calculated from the Arrhenius dependences correspond to 0 K. These energies, which were calculated from the slope of the experimental CVC (see Fig. 15), depend on the electric field (see Fig. 16), which is also a manifestation of the Poole-Frenkel effect.



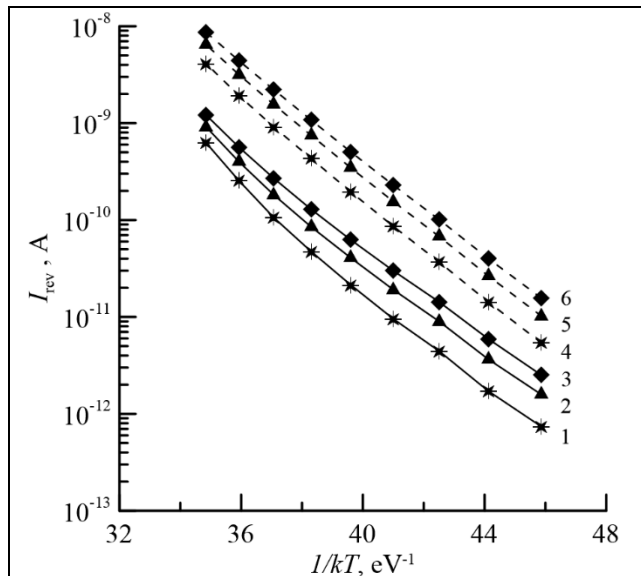


Fig. 15: Temperature dependences of the reverse current before irradiation (1-3), and after (4-5) at voltages, V: 1.4 -10; 2.5 -20; 3.6-30.

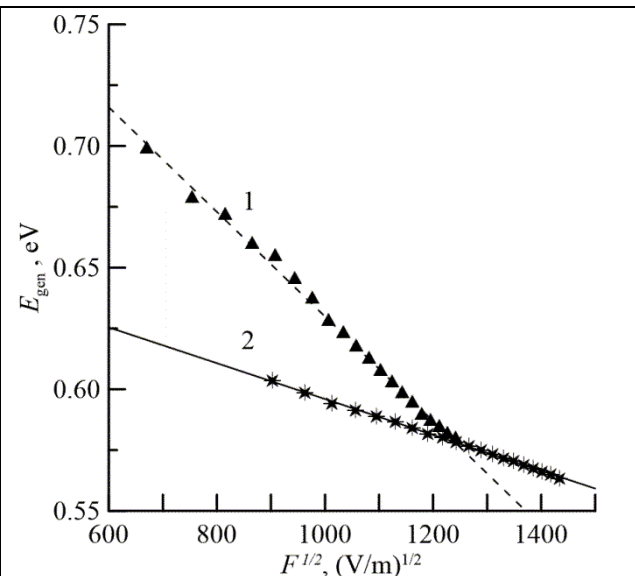


Fig. 16: Change in the activation energy of the generation process depending on the electric field: 1 - before irradiation; 2 - after irradiation.

The experimental data presented show that the generation and recombination processes involving recombination centers determine the magnitude of the forward and reverse currents of the diodes. We will determine the parameters of these centers from the CVC.

At reverse voltage, the SCR of the p-n junction is depleted in free charge carriers; the equilibrium between recombination and generation is shifted toward generation. The reverse current is determined by the expression:

$$I_{rev} = qA \int_0^w R dx \tag{7.1}$$

Where: R is the generation rate. In the case of generation with the participation of the recombination center (RC), which has one deep level in the band gap of these semiconductor, its rate can be found from the system of kinetic equations:

$$\begin{aligned} R_n &= \frac{dn}{dt} = -c_n n(N_t - n_t) + e_n^t n_t \\ R_p &= \frac{dp}{dt} = -c_p p n_t + e_p^t (N_t - n_t), \end{aligned} \tag{7.2}$$

Where: n_t is the concentration of electrons on RC. When calculating the generation rate, it is taken into account that in the equilibrium position, we get:

$$I_{rev} = qA \int_0^w \frac{e_n^t(x)e_p^t(x)N_t(x)}{e_n^t(x) + e_p^t(x)} dx, \tag{7.3}$$

Where: $e_n^t = \gamma_n c_n N_c \exp(-(E_C - E_t)/k_B T)$,

$e_p^t = \gamma_p c_p N_v \exp(-(E_t - E_V)/k_B T)$; γ_n , γ_p are the degeneration factors of the deep center level for electrons and holes. These factors vary from 0.5 to 2.

It should be noted that the rate of thermal emission depends on the temperature exponentially, therefore, if the RC level differs from the middle of the band gap by $(3 - 5)kT$, then, as a rule, the rate of emission of electrons or holes is much higher than the rate of another transition. We make the following approximations: the recombination level is located closer to the conduction band; RCs are evenly spaced across the SCR; thermal emission rates are independent of the electric field. It turns out a simple expression for the reverse current of the diode:

$$I_{rev} = qAw(U)N_t e_p^t \tag{7.4}$$

Eq. (7.4) includes the emission rate of holes, not electrons, since the magnitude of the current at reverse bias is determined by the slowest process, namely, the emission rate with higher activation energy. Therefore, in the case of thermal generation through the RC, the energy experimentally obtained is more than half the band gap. Accordingly, the energy of the recombination center at zeroelectric field strength ($E_t(0)$) is related to the activation energy of the generation process (E_{gen}) by the expression:

$$E_t(0) = E_g(0) - E_{gen}(0). \tag{7.5}$$

Eq. (7.4) shows that the generation current at reverse bias is directly proportional to the concentration of recombination centers and has voltage dependence, however weak. Therefore, it grows after irradiation. Eq.

(7.5), as a first approximation, correctly describes the temperature dependence of the current (see Fig. 14), however, this formula gives a dependence of the current on the reverse bias voltage by square or cubic root, which is due to a change in the width of the depletion region, and it does not follow that the activation energy of hole emission depends on the voltage. The experimentally measured current (see Fig. 14) varies exponentially from the reverse bias voltage, which is due to a change in the probability of emission depending on the electric field strength in the SCR of the p-n junction. Lowering the height of the potential barrier due to the Pool-Frenkel effect[15] has the form:

$$\Delta E_t = \frac{q^{3/2}}{\sqrt{\pi\epsilon\epsilon_0}}\sqrt{F} = \beta_F\sqrt{F} . \tag{7.6}$$

The factor in front of the root of the electric field, which is called the Frenkel constant ($\beta_F = q^{3/2}/\sqrt{\pi\epsilon\epsilon_0}$), does not depend on the technological parameters of the device, but is determined only by constants. Its value is in practical units $0.00023 \text{ eV}\cdot\text{cm}^{1/2}/\text{V}^{1/2}$. With the help of formula (7.6), the expression for the CVC of the p-n junction at reverse bias is calculated:

$$I_{rev} = qAe_{p0}^t \int_0^w N_t(x) \exp\left(\frac{\Delta E_t(x)}{kT}\right) dx = qAe_{p0}^t \int_0^w N_t(x) \exp\left(\frac{\beta_F\sqrt{F(x)}}{kT}\right) dx , \tag{7.7}$$

Where: e_{p0}^t is the hole emission rate without taking into account the influence of the electric field.

Eq. (6.7) takes into account the effect of both temperature and electric field strength. The energy of the generation process taking into account the Poole-Frenkel effect is:

$$E_{gen}(F) = E_{gen}(0) - \beta_F\sqrt{F} , \tag{7.8}$$

Where: $E_{gen}(0)$ is the energy of the generation process in the absence of an electric field.

This dependence in coordinates $E_{gen}(F) = f(F^{1/2})$ looks like a straight line. The approximation of the experimental results in Fig. 16 has the same form, which makes it possible to determine the energy of the generation process in the absence of an electric field ($E_{gen}(0)$) and the experimental value of the Frenkel constant (β_{Fex}). These parameters are shown in Table 2. The electron-phonon interaction leads to the fact that the defect must be characterized by several parameters, and not by one activation energy.

Table 2: Parameters of generation centers, which determine the reverse current before and after irradiation

Experimental and calculated parameters	β_{Fex} , eVcm ^{1/2} V ^{1/2}	$E_{gen}(0)$, eV	$E_t(0)$, eV	$S\hbar\omega$, eV	E_0 , eV	ΔE , eV
Before irradiation	$21.5 \cdot 10^{-4}$	0.85	0.32	0.003	0.063	0.46
After irradiation	$7.4 \cdot 10^{-4}$	0.67	0.50	0.045	0.254	0.17

Note: The energy $E_t(0)$ was calculated using formula (19). For silicon $E_g(0) \approx 1.17 \text{ eV}$. The values of the parameters $S\hbar\omega$ and E_0 were calculated from the joint solution of equations (6.3) and (7.9). The values β_{Fex} , $E_{gen}(0)$, ΔE were found from the experiment.

In our case, the experimental values β_{Fex} are several times higher than the theoretical ones, which is associated with the electron-phonon interaction. In the work by S.F. Timashev, it is shown [24] that:

$$\beta_{Fex} = \beta_F \left(1 + \frac{E_0 - S\hbar\omega}{2S\hbar\omega} \right) \tag{7.9}$$

Eq. (7.8) and (7.9) allow calculating the parameters of the electron-phonon interaction $S\hbar\omega$ and

E_0 . These parameters are given in Table 2. The value of the experimental Frenkel constant and the thermal activation energy of the generation process in the absence of an electric field $E_t(0)$ are calculated from the experimental data shown in Fig. 16. The results of calculations are presented in Table 2. These parameters, as well as the energy of thermal activation $E_t(0)$, after irradiation take on different values (Table 2). The data given in Table 2 allow us to construct the configuration-coordinate diagrams of the centers, which determine the magnitude of the reverse currents of the p-n junction before and after irradiation. They are shown in Fig. 17.

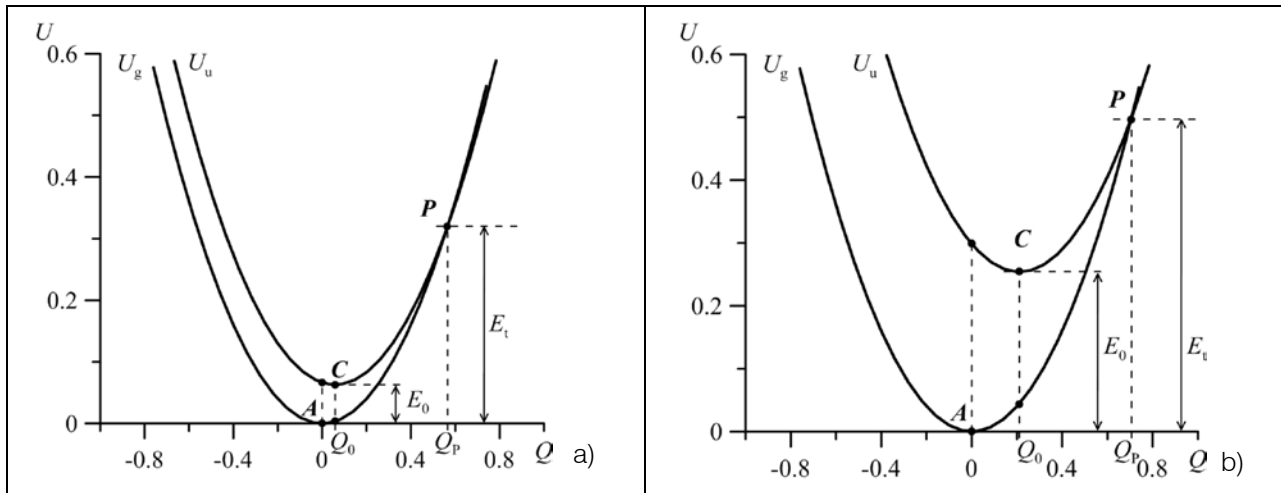


Figure 17: Configuration-coordinate diagrams of recombination centers:
 a) before irradiation; b) after irradiation [16]

These diagrams differ in the energies of purely electronic transitions and in the polar on shift, which also indicates a change in the nature of the recombination center after irradiation. The activation energies ΔE for the capture of charge carriers by the recombination center in the classical one-coordinate model and at high temperatures are related to the thermal activation energy $E_t(0)$ and the purely electronic transition energy E_0 : $\Delta E = E_t(0) - E_0$. At lower temperatures, the energy E decreases because capture occurs by a tunneling method, rather than activation through a barrier with a maximum at point P . In our case, ΔE agrees with the difference between the thermal activation energy of the RC and the energy of a purely electronic transition.

The polar on shift (Q_0) and the activation energies of capture to there combination center differ before and after irradiation. The polar on shift before irradiation is smaller, the capture energy is higher than after irradiation, which indicates that the electron-phonon interaction is less pronounced before irradiation. The electron-phonon interaction, as a rule, manifests itself more strongly in molecular objects; therefore, it can be assumed that the nature of the recombination centers found in this work is associated with molecular complexes of a silicon vacancy with an impurity and is consistent with the conclusions of Section 2, according to which, after irradiation, the V2O center appears. It is known that at high irradiation doses in silicon diodes, there are processes associated with the meta stability of such centers and with the Jahn-Teller effect, which are inherent in them [25,26], which is also a manifestation of the electron-phonon interaction.

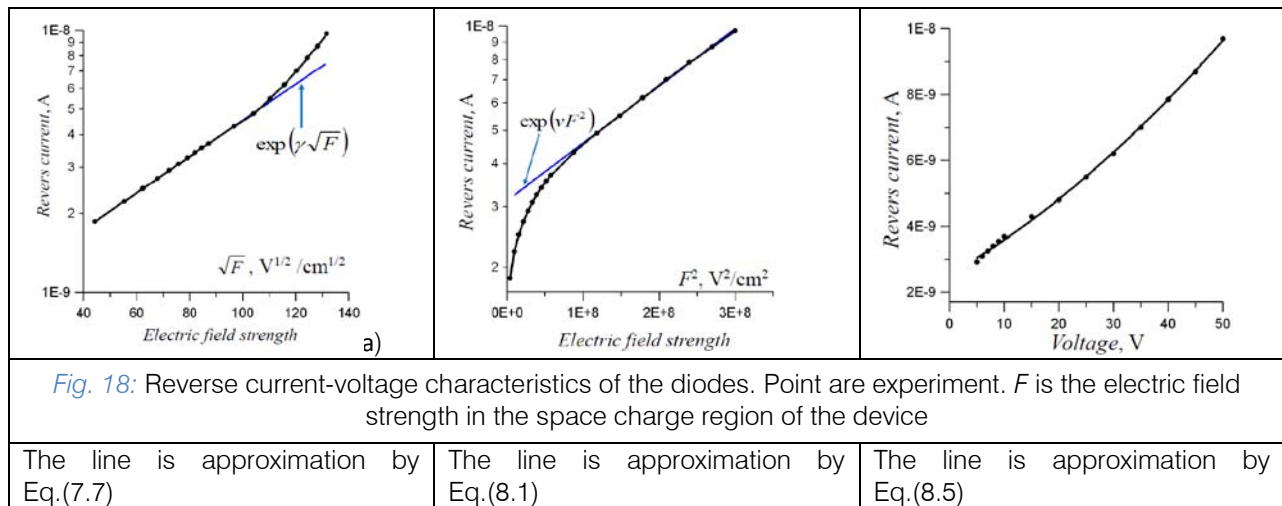
The experimental results of measuring the reverse currents agree with the analysis of the recombination currents, which show that irradiation results in the formation of centers of two silicon vacancies with oxygen, which also determine the

magnitude of the reverse currents of diodes. In this case, the generation of charge carriers is influenced by the electron-phonon interaction. We have developed a technique for determining the parameters of this interaction from the reverse CVC.

VII. CALCULATION OF THE MAGNITUDE OF THE REVERSE CURRENTS OF P-N-JUNCTIONS TAKING INTO ACCOUNT THE INFLUENCE OF ELECTRON-PHONON INTERACTION ON THE GENERATION OF ELECTRONS AND HOLES IN STRONG ELECTRIC FIELDS

a) Poole-Frenkel effect

The electric field leads to a decrease in the height of the potential barrier for the generation of an electron or a hole from a deep center to one of the allowed bands. This phenomenon is called the Poole-Frenkel effect and leads to an increase in reverse current as the voltage across the diode rises. The change in the current is is described by the formula (7.7), the lowering of the potential barrier is shows (7.8). The Frenkel constant taking into account the electron-phonon interaction can be calculated by the formula (7.9). The calculation results using these formulas are shown in Figure 18 a. The data in Table 1 were used for the calculation.



The calculation result describes the change in the reverse current in the region of low and medium electric field strengths. At high field strengths, the current increases faster than predicted by dependence (7.7), even taking into account the electron-phonon interaction. We can conclude that the mechanism for the generation of electrons and holes is more complex and that not only the Poole-Frenkel effect but also other phenomena are involved in its formation.

b) Refinement of the Poole-Frenkel theory

Timashev came to the conclusion that localized states appear in a strong electric field near the allowed bands [24]. Thermal generation is complemented by the tunneling of electrons and holes to these states, and then the charge carriers pass into the allowed conduction and valence bands. Tunneling increases the likelihood of thermal generation. Franz and Keldysh predicted this earlier for optical transitions [11]. Timashev obtained the following expressions for the rate of thermal emission taking into account the strong electric field and electron-phonon interaction, which were experimentally confirmed in [7]

$$e_n^t = e_{n0}^t(0) \exp(\gamma F^{1/2} + \lambda F^2) \quad (8.1)$$

Where: $\gamma = \beta_F \left[1 + \frac{(E_{p0} - \hbar\omega)kT}{\sigma^2} \right]$; $\lambda = \frac{1}{24} \left[1 + \frac{(E_0 - \hbar\omega)kT}{\sigma^2} \right] \frac{q\hbar^2}{m_n^*(kT)^3}$

The first term in the exponent describes the Poole-Frenkel's effect, and the second additional increase in the rate of thermal emission in a strong electric field. Current-voltage characteristic should be linear in the coordinates $\ln(I_{rev}) = f(F^2)$, which is observed experimentally (Fig. 18b). This result confirms the influence of the electron-phonon interaction, which accelerates the processes of emission in an electric field (Eq.(8.1)). Eq. (8.1) there is a good description of the change in the reverse current in a strong electric field, but this approximation is worse at low field strengths.

c) Quantum-mechanical calculation of the probability of an electronic-vibration transition from localized states of deep centers

The calculation of the probability of electronic transitions with the participation of deep centers must be performed taking into account the interaction of an electron or hole with lattice vibrations. Transitions between energy states are called electronic-vibration in this case.

There are two difficulties that are associated with the calculation of such transitions. The first is related to the calculation of the wave functions of the electrons localized at the center. This is a difficult task. It is solved by applying model representations for the wave functions of the deep center. The second difficulty is associated with a lack of information about the nature of the electron-phonon interaction, which has a significant impact on the speed of electronic transitions.

These problems were overcome in works [12, 13]. The expression for the probability of a quantum-mechanical transition, taking into account the electron-phonon interaction, can be written in the form in accordance with this Eq. (3.4)

Eq. (3.4) is written for a situation where the energy spectrum consists of two groups of close levels $(1; 2_j)$ separated by a large energy gap. Let the electron transition be between singlet states, then:

$$W_{n,p}(F, T) = \int_{-\infty}^{\infty} W_{0n,p}(E_{t,n,p} - \epsilon) f_{n,p}(\epsilon) d\epsilon \quad (8.2)$$

Eq. (8.2) is a generalized expression for the probability of an electronic transition, which allows us to calculate the dependences of the probabilities of electronic-vibration transitions on the electric field strength and temperature and not use the single-coordinate model. Such an approach makes it possible to avoid simplifying the complex interaction of electrons with a lattice. This expression can be used for multiphonon on thermal, tunnel, and optical transitions. Eq. (8.2) can be used when the formula of a purely electronic

transition is the formula that expresses this mechanism. In the first approximation, we consider that a purely electronic transition is a tunnel one, and the Gauss function is the form-function of the electronic-vibration transition. The probability of a tunnel junction for tunneling through a potential triangular barrier has the form [13]:

$$W_{0n}(E_{ii} - \varepsilon) = \frac{eF}{2\sqrt{2m^*(E_m - \varepsilon)}} \exp\left(\frac{4(E_m - \varepsilon)^{3/2}\sqrt{m^*}}{3\hbar eF}\right) \quad (8.3)$$

Where: $E_{m,p}$ there is the energy of a purely electronic transition from the deep level to the conduction band or the valence band; F is the electric field strength; $f_{n,p}(\varepsilon)$ is a form-function of an electronic-vibration transition. The form-function is:

$$f_{n,p}(\varepsilon) = \frac{1}{\sigma\sqrt{2\pi}} \exp\left(-\frac{(\varepsilon - E_{m,p})^2}{2\sigma^2}\right) \quad (8.4)$$

The transition probability Eq. (8.9) is equal to the thermal emission rate in Eq. (8.3), then the expression for the reverse current of the diode is:

$$I_{rev} = eS w N_i W_{n,p}(F, T) \quad (8.5)$$

The magnitude of the reverse current of the diode was calculated from Eq. (8.5), taking into account Eq. (8.2) - Eq. (8.4), as well as the data presented in Table. 1. Moreover, we take into account the parameters of transition of holes from the valence band to the level of a recombination center with an energy of 0.53 eV, since this center is located near the middle of the silicon band gap. The calculation results are compared with the

$$\alpha f_{abs}(h\nu) + \int_a^b k(h\nu, s) f_{abs}(s) ds = w(h\nu), \quad a \leq h\nu \leq b, \quad (8.8)$$

Where: $k(h\nu, s) = \int_c^d K(t, h\nu) K(t, s) dt$, $w(h\nu) = \int_c^d K(t, h\nu) W_{abs}(t) dt$, $K(x, y) = \begin{cases} \sqrt{x-y}, & n\mu x > y \\ 0, & n\mu x < y \end{cases}$

a, c and b, d here are the lower and upper energy boundaries of the range of measured photoionization rate spectra. The calculation results are shown in table 4.

Table 4: Parameters of the electron-phonon interaction of the EL2 trap

	S	$\hbar\omega_{u, \text{эB}}$	$\hbar\omega_{g, \text{эB}}$	$E_0, \text{эB}$
EL2→E _c	7	0.020	0.019	0.73
E _v →EL2	7	0.021	0.018	0.74

experiment in Fig. 18c. The results of the calculation and experiment are in agreement between themselves, which proves the calculations are correct.

The parameters of the electron-phonon interaction can be calculated from experiments on luminescence and light absorption [12, 13]. The EL2 trap plays an important role in gallium arsenide devices. In this regard, relying on the results of [27-29], we will estimate the parameters of the electron-phonon interaction of this trap.

For the calculations, the spectra of the photoionization and absorption cross sections, which are given in [16, 19], and the following algorithm for obtaining the parameters of the electron-phonon interaction were used. The photoionization cross sections for electrons of the recombination center are described by the expression:

$$q_n(h\nu) = G_0 \int_{h\nu-\Delta}^{h\nu} \sqrt{h\nu - \varepsilon} f_{abs}(\varepsilon) d\varepsilon \quad (8.6)$$

To find the form-function of optical absorption $f_{abs}(h\nu)$, it is necessary to solve equation (8.6), which is the Fredholm integral equation of the first kind. This equation is solved with respect to quant energy $h\nu$ using the integral Riemann-Liouville transformation [12.13]:

$$f(h\nu) = \frac{4}{G_0} \frac{d}{dh\nu} \left\{ \int_{-\infty}^{h\nu} \frac{q_n'(\xi) d\xi}{\sqrt{h\nu - \xi}} \right\} = \frac{4}{G_0} D^{1/2} \{q_n'(h\nu)\}, \quad (8.7)$$

Where: $D^{1/2}$ is the fractional derivative of degree 1/2. The sought-for form-function was calculated using the Tikhonov's 0th order regularization method, according to which the problem was reduced to solving a system of linear equations:

These parameters were used to calculate the reverse current of Ga As-based diodes. The calculation results are shown in Figure 19.

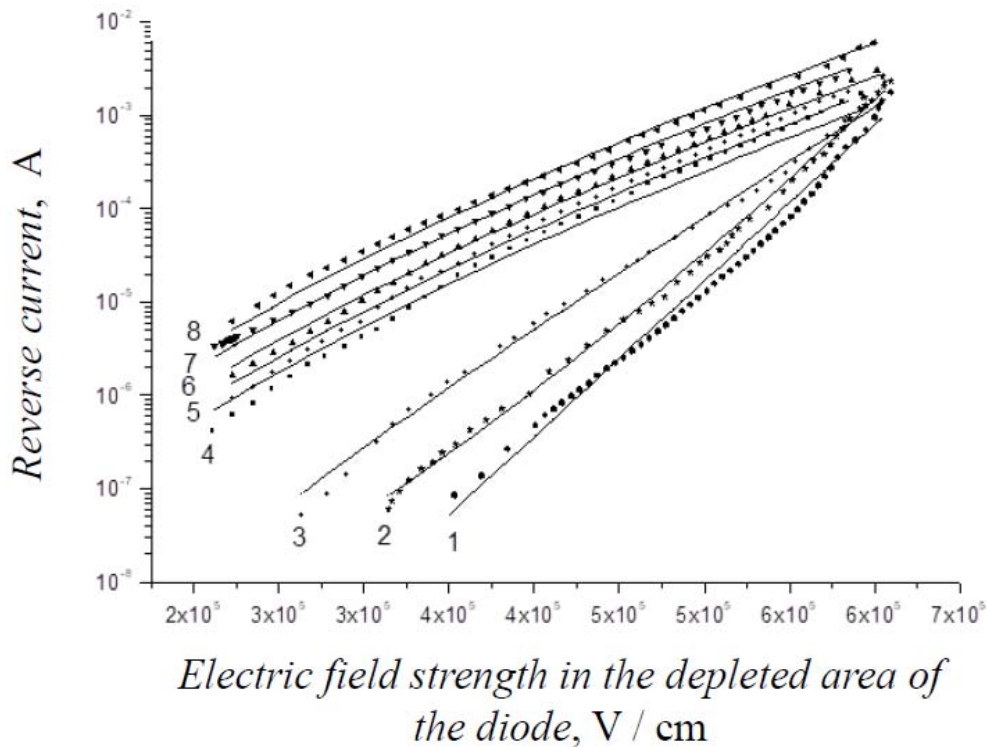


Figure 19: Experimental backward I - V characteristics of p - n junctions based on GaAs (points) and calculation using formula (8.5) (solid lines) at temperatures, K: 1 - 88; 2 - 170; 3 - 230; 4 - 295; 5 - 303; 6 - 313; 7 - 323; 8 - 333.

The calculation results are in good agreement with the experiment. This proves the adequacy of the theory that is developed in this article, and shows that to calculate the form function, you can use various experiments, and then calculate the magnitude of the reverse currents of semiconductor devices.

VIII. CONCLUSION

We have developed new approaches to generation-recombination processes in semiconductor materials and devices. Two important factors were taken into account when developing a new recombination model: localization and electron-phonon interaction. The model of exchange between localized states combines generation-recombination processes and charge carrier transport. Therefore, it can be applied to semiconductors with nanostructured ordering and combines the Shockley recombination model with the Mott hopping conductivity model and tunneling. It implies the model of tunnel recombination, which is used in a sufficiently large number of semiconductor structures. We demonstrate the success of this model on the any examples. Thus, we have obtained formula) for the exchange rate between neighboring localized areas. This formula allows you to study the complex transfer mechanisms. It combines such important

mechanisms as the Shockley recombination model and the Mott hopping conductivity.

We have developed a model of electron-vibrational transitions of electrons and holes from deep levels to allowed zones, and an expression is obtained for the probability of such a transition from first principles. The results is shown the leading role of the electron-phonon interaction in the ionization of deep centers.

The theory of recombination in the space charge region of semiconductor devices was further developed in this work. The method for determining the parameters of the recombination centers is developed. It is called recombination spectroscopy. This method allows you to determine the activation energy and lifetimes at a constant temperature, including at room temperature. It is simple from the point of view of measurements. It uses standard equipment and allows automation of the determination of the parameters of deep centers. Moreover, it allows measurement directly on a semiconductor wafer, before sorting out semiconductor structures and cutting the wafer into individual crystals.

The calculations and experiments that were performed in this article show the drawbacks of simple classical formulas for describing recombination and generation processes in semiconductor p-n-junctions.



The ideality factor is not constant and depends on the recombination fluxes of electrons and holes, which change as a result of injection. Algorithms for converting current-voltage characteristics are taking place. These algorithms allow one to estimate the parameters of the recombination centers when the temperature of the experiment does not change. Processing current-voltage characteristics together with measurements of the capacitance of p-n-junctions allow us to calculate a large set of parameters of the recombination centers, including the parameters of the electron-phonon interaction. The electron-phonon interaction leads to the fact that the reverse current of p-n-junctions increases with increasing voltage faster, which is predicted by the Poole-Frenkel's theory. This is proved by the calculations and experiments that are carried out in this article. General considerations of a physical nature suggest that the electron-phonon interaction should be stronger when the recombination centers are molecules of the type of complexes of a vacancy with an impurity. Such centers may be weakly associated with the main lattice, and in this case the vibrations of the main lattice less suppress the molecular vibrations inside such centers.

ACKNOWLEDGEMENTS

This work was supported by the Ministry of Science and Higher Education of the Russian Federation, project No. 0004-2019-0001.

REFERENCES RÉFÉRENCES REFERENCIAS

- Shokley W. The theory of p-n-Junction in semiconductor and p-n-Junction transistors.// Bell Syst Tech 1949; 28:435.
- Sah CT, Noyce RN, Shockley W. Carrier generation and recombination in p-n junctions and p-n junction characteristics. //Proc IRE 1957; 45(9):1228–43.
- Sah CM, Forbes A. Thermal and optical emission and cross section of electrons and holes at imperfection centers in semiconductors from photo dark junction current capacitance experiment. // Sol State Electron 1970: 13.758-769.
- Pichler P. "Intrinsic point defects, impurities, and they diffusion in silicon", Springer-Verlag, 2004. 554 p.
- S. V. Bulyarskiy, N. S. Grushko Generalized Model of Recombination in Inhomogeneous Semiconductor Structures.//Journal of Experimental and Theoretical Physics, 2000; 91, No. 5, 1059–1065.
- S. V. Bulyarskiy, Yu. V. Rud', L. N. Vostretsova, A. S. Kagarmanov. O. A. Trifonov. Tunneling Recombination in Semiconductor Structures with Nanoscale Disorder. Semiconductors, 2009, Vol. 43, No. 4, pp. 440–446.
- Bulyarskiy SV, Grushko NS, Gudkin AA. Field dependences of thermal ionization of deep centers in the space charge layer of Au – n-InP: Fe barriers. Semiconductors1975;9:287–91.
- Makram-Ebeid S. Effect of electric field on deep-level transients in Ga As and GaP. Appl PhysLett 1980;37(5):464–70.
- Makram-Ebeid S, Lannoo M. Quantum model for phonon assisted tunnel ionization of deep levels in semiconductors. Phys Rev 1982; 25(10):1082–90.
- Perel Karpus VI. Multiphonon ionization of deep centers in semiconductors in anelectric field. J Exp Theoretical Phys 1986;64:1376–91.
- Ridley B. Quantum Processes in Semiconductors. 2nd ed. Oxford: Clarendon Press; 1988.
- Bulyarskiy SV, Grushko NS, Zhukov AV. Calculation of the field dependence of therates of emission of carriers from deep centers based on an experimental form function for the optical transition. J. Exp. Theor. Phys 1999;89(3):547–51.
- Bulyarskiy SV, Grushko NS, Zhukov AV. Calculation of the probability of nonradiativeelectronic transitions from deep centers in GaAs in the one-coordinate approximation.// Opt Spektrosk 2001;90(3):440–5.
- S. V. Bulyarskiy, A. V. Zhukov, O. S. Svetukhina, O. A. Trifonov. Effect of Stationary Ionization of Traps Near the Midgap on the Spectrum of Thermally Stimulated Capacitance of Semiconductor Devices// Semiconductors, 2006, Vol. 40, No. 9, pp. 1105–1108
- S. V. Bulyarskiy The effect of electron-phonon interaction on the formation of reverse currents of p-n-junctions of silicon-based power semiconductor devices.//Solid State Electronics 160 (2019) 107624. doi.org/10.1016/j.sse.2019.107624.
- S. V. Bulyarskiy, A. V. Lakalin, M. A. Saurov, G. G. Gusarov. The effect of vacancy-impurity complexes in silicon on the current-voltage characteristics of p-n junctions// J. Appl. Phys. 2020. DOI: 10.1063/5.0023411/
- S. V. Bulyarskiy, N. S. Grushko, A. I. Somov, A. V. Lakalin. Recombination in the space charge region and its effect on the transmittance of bipolar transistors.// 1997 American Institute of Physics.@S1063-7826~97102509-X#. Semiconductors 31 (9), September 1997.
- S. V. Bulyarskiy, N. S. Grushko, A. V. Lakalin. Differential methods for determination of deep-level parameters from recombination currents of p –n junctions.// 1998 American Institute of Physics, 1063-7826/98/32, Semiconductors 32 (10), October 1998.
- S. V. Bulyarskiy, M. O. Vorob'ev, N. S. Grushko, A. V. Lakalin Deep-level recombination spectroscopy in GaP light-emitting diodes//1999 American Institute of Physics, 1063-7826/99/33(6)/4/, Semiconductors 33 (6), June 1999.

20. S. V. Bulyarskiy, Determination of the parameters of deep levels from the relaxational delay of breakdown of a p–n junction//1999 American Institute of Physics, 1063-7826/99/33(4)/4. Semiconductors 33 (4), April 1999.
21. S. V. Bulyarskiy , M. O. Vorob'ev, N. S. Grushko, and A. V. Lakalin Determination of the parameters of deep levels using the differential coefficients of the current–voltage characteristics//1999 American Institute of Physics, 1063-7850/99/25(3)/3/. Tech. Phys. Lett. 25 (3), March 1999.
22. S. V. Bulyarskiya, A. V. Lakalin, I. E. Abanin, V. V. Amelichev, and V. V. Svetuhin. Optimization of the Parameters of Power Sources Excited by β -Radiation// Semiconductors, 2017, Vol. 51, No. 1, pp. 66–72.
23. Timashev SF. On the Frenkel effect during thermofield ionization of deep centers in the space charge layer in semiconductors. Phys Solid State 1974;16:804–811.
24. L. I. Murin, V. P. Markevich, I. F. Medvedeva, L. Dobaczewski. Bistability and Electrical Activity of the Vacancy–Dioxygen Complex in Silicon. Semiconductors, 2006, Vol. 40, No. 11, pp. 1282–1286.
25. S. B. Lastovskii, V. P. Markevich, H. S. Yakushevich, L. I. Murin, V. P. Krylov. Radiation-Induced Bistable Centers with Deep Levels in Silicon n+–p Structures// Semiconductors, 2016, Vol. 50, No. 6, pp. 751–755.
26. Silverberg P., Omling P. Samuelson L. Optical cross sections of the two energy levels of EL2 in GaAs // Paper present. At 5th Conf. On Semi-insulating III-V materials. Malmo. Sweden. 1988. P. 369.
27. Reddy C.V., Fung S. and Beling C.D. Nature of the bulk defects in GaAs through high-temperature quenching studies //Phys. Rev.B. V.54, 11290.
28. Bagraev N. T. The EL2 center in GaAs: symmetry and metastability//J.Phys. I France 1 (1991) P. 1511-1527.